Jurnal Kejuruteraan 33(4) 2021: 1037-1044
https://doi.org/10.17576/jkukm-2021-33(4)-25

# Improvement in Corrosion Resistance of Magnesium-Aluminum Alloy Via Friction Stir Processing

Minal S. Dani[a*], I.B. Dave[a] & Alphonsa Joseph[b]

[a]*Metallurgy department, Government Engineering College, Sector- 28,Gandhinagar 382028, Gujarat, India,*
[b]*Facilitation Centre for Industrial Plasma Technologies (FCIPT), Sector-25,Gandhinagar 382016, Gujarat, India*

**Corresponding author: minal@gecg28.ac.in*

*Received 31March 2021, Received in revised form 07May 2021*
*Accepted 08June 2021, Available online 30 November 2021*

ABSTRACT

*Friction stir processing was done for surface modification of cast Magnesium-Aluminum alloy. The microstructural characteristics related to different phases of untreated cast Magnesium-Aluminum alloy, friction stir processed under different process parameters like rotational speeds at 380rpm and 545 rpm with 31.5 mm/min transverse speed with and without pure aluminum powder were investigated by Metallurgical microscopy at lower magnification and scanning electron microscopy at higher magnification. Pure aluminum powder of fine size (~19µm) was filled in the groove made at the center of the Magnesium-Aluminum alloy plate which cover 33 vol% of pure aluminum during friction stir processing. The electrochemical behavior of the Magnesium-Aluminum alloy, Friction stir processed Magnesium-Aluminum alloy without aluminum powder and Friction stir processed Magnesium-Aluminum alloy with pure aluminum powder were investigated using Potentiostat in 5 wt % sodium chloride (NaCl) solution.Surface of all conditions specimens were analyzed for the phases present on the surface by X-Ray Diffractometer (XRD) which revealed different peaks of α-Mg phase, β-phases (Mg17Al12) and Pure Aluminum . In friction stir processed Magnesium-Aluminum alloy double pass with aluminum powder all these peaks were observed. The electrochemical corrosion tests revealed the least corrosion rate (0.603 X 102mpy) for friction stir processed double pass with aluminum powder amongst all the tested specimens. The improvement in corrosion resistance of friction stir processed double pass with aluminum powder is because of more formations of the β-phases (Mg17Al12) and aluminum dissolved in the α-Mg phase.*

*Keywords: Magnesium-aluminum alloy, surface modification, friction stir processing, electro chemical corrosion, β-phases (Mg17Al12)*

## INTRODUCTION

The significance of Magnesium (Mg) alloys has accelerated in wide industrial applications due to the light in weight with good strength, fair measurement stability, suitable machining and the good potential to be recycled (Emley 1966). The need for weight reduction, mainly in microelectronics, telecommunication, aerospace and vehicles has stimulated the engineers to be adventurous in choosing the right materials (Ambat et al 2000). However, the Magnesium alloys have poor corrosion resistance which is major problem which prevent their use in outdoor usage because of their high reactivity compared to steel and aluminum alloys. For aeronautical applications, where excessive mechanical properties are needed, Magnesium alloys are considered only if they have a fine-grained structure which developed due to high strength and ductility combinations at room temperature via grain refinement (Kubota et al. 1999). Furthermore, high quality fine grained Mg-based alloys showcase superplastic behavior at excessive strain rates ($\geq 10^{-1}$ $s^{-1}$) and low temperatures ($\leq$473 K) (Abdelaziz et al. 2017). Recently, for preparation of magnesium alloys, Friction stir Processing (FSP) is being used as a promising approach for limitation of defects, homogenization and grain refinement. (Gandra et al. 2011, Nia et al. 2014) Moreover, the corrosion rate of Mg alloys can also be minimized during friction stir processing by producing surfaces strengthened by intermetallic phases (Chang et al. 2007).

On work piece nonconsumable tool was rotated along

working direction and due to friction between rotating tool and workpiece, friction stir processing (FSP) is carried out. FSP work depends on tool shoulder diameter and tool pin depth. During FSP, when the rotating tool is introduced into workpiece, the shoulder diameter of tool size was occupied the surface of the workpiece which deform the material plastically due to generation of frictional heat created by rotational speed (Dani et al. 2019, Ahmadkhaniha et al. 2016, Patel et al.2018, Sharma et al. 2021). Surface modification by FSP thus depends on rotational speed, transverse speed, number of passes, tool geometry and tool tilt angle. Hence, due to the dynamic recrystallization of the deformed zone within the material, the ultrafine grain structure is formed (DU et al. 2008, Li et al 2019, Patel et al. 2019) It has been established by many researchers that, in FSPed Mg alloys, reduced grain size led to improvement in properties like ability to form, ductility and resistance to corrosion, hardness and strength without affecting the major alloys properties (Hütter et al. 2016). Numerous studies have shown that, there was an improvement in the strength, hardness and resistance to corrosion and wear after reinforcements have been added to the base metal during FSP (Khodabakhshi et al. 2017, Li, PL et al. 2019, Patel et al. 2019, Akinwekomi 2018, Dani et al. 2019,Ahmadkhaniha et al. 2016). Adentula et al. used four special powders (Fly ash, Ash of Palm Kernel Shell, Austenitic stainless steel 304 grade and Titanium alloy grade Ti-6Al-4V powders) as reinforcements in Mg alloys during FSP to improve corrosion resistance along with mechanical properties like hardness, tensile strength and wear resistance (Adetunlaet al 2016, Akinlabi et al. 2018). Furthermore, SiC, SiO2 and C60 has also been as reinforcements on cast Mg alloy substrates (MORISADA 2006), while manufacturing surface composites via FSP, prepared, an Al-rich surface layer utilizing aluminum powder in thixoformed AZ91D alloy for enhancing their corrosion resistance properties by the usage of the FSP method (Chen et al. 2007) .This improvement was mainly attributed to the increasing aluminum concentration in the α-Mg phase as well as more formation of β-phases ($Mg_{17}Al_{12}$)(Chen et al. 1999,Chen et al. 2009, Song et al. 1998, Song et al. 1999, Dani et al. 2019).

Almost very negligible work has been done on FSP using pure aluminum (Al) powder as reinforcement material on Magnesium-Aluminum alloy. In this research, main focus is to improve the resistance to corrosion of Magnesium-Aluminum alloy using aluminum powder under various rotation speeds and passes by FSP. An attempt has been made to study and compare the corrosion behavior in 5 wt % NaCl solution of the Magnesium-Aluminum alloy along with FSP treated Magnesium-Aluminum alloy under different process conditions, with and without aluminum powder.

## EXPERIMENTAL WORK

In this research work, Magnesium-Aluminum alloy which was manufactured by die casting method were used containing Alumnium-9.65 %; Zinc-0.772%, Manganese-0.027%; and balance Mg which was similar to AZ91 Mg alloy (SONG G et al. 1998). On this Magnesium-Aluminum alloy (9 % Aluminum), FSP was done with and without Al powder, at 380 rpm and 545 rpm rotational speeds. A transverse speed of 31.5 mm/min and a tool tilt angle of 30 was maintained for single and double passes. Non-consumable taper threaded tools made of H13 grade tool steel with pin (3 mm diameter and 5 mm length) and shoulder diameter of 18 mm were used for FSP as shown in Figure 1.

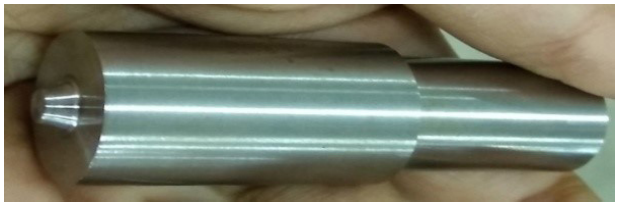

FIGURE.1: H13 grade non consumable tool used for FSP

Pure aluminum powder of a fine size (~19μm) was filled in the groove of 2 x 2 x 150 mm, which was made by a CNC machine at the center of the Magnesium-Aluminum alloy plate. FSPed four specimens were made with 380 rpm with and without Al powder during single passes (SP) and double passes (DP). Similarly, another four specimens were also made with 545 rpm with and without Al powder during SP and DP. There was no sticking of Mg around the tool at 380 rpm and 545 rpm rotational speeds. Thus, eight different specimens were produced by FSP and their corrosion behavior was compared with the untreated specimen.

The FSPed specimens treated under various conditions were observed by Scanning Electron Microscopy (SEM) to study the morphology on the composite surface. Also, the surface of the specimens was analyzed for the phases present on the surface using a German make "Bruker" XRD. XRD have Cu- Kα radiation( $\lambda = 1.5406$ A$^o$), 40 KV, 40 mA with 0.05 step size/ scan speed using Bragg- Branteno powder mode. The 2θ scan range was from $10^0$ to $90^o$. The resultant scan data was analyzed using Diffract.eva softwarewith the ICDD database.

The friction stir processed specimens were cross sectioned perpendicular to FSP direction for specimen preparation. Before the corrosion test, specimens were wet ground with grade P1200 grit emery paper for smooth surface finish followed by drying in warm air. In all cases, the corrosion tests were performed in duplicate to guarantee the reliability of the results. The electrochemical

measurements were performed on Magnesium-Aluminum alloy and FSP treated specimens prepared under various rotational speeds during single and double passes at Facilitation Center for Industrial Plasma Technologies (FCIPT), Gandhinagar, Gujarat, India. The working area of the specimens were 0.785cm²and were exposed to 5wt % NaCl solution at room temperature (25°C). A Gamry make Reference 600 potentiostat connected to three electrodes was used for the corrosion studies. In the three-electrode system, the working electrode was the test specimen. Platinum and the Standard calomel electrode (SCE) were used as a counter electrode and reference electrode respectively. The potentiodynamic polarization curves were measured after stabilization for 30 min to obtain open circuit potential (OCP). The cathodic polarization scan started from -500mVwhich was followed by 1 milivolt per second anodic scan for potentiodynamic polarization measurements.

## RESULT AND DISCUSSION

### SURFACE MORPHOLOGY OF UNTREATED CAST AND FSPED MAGNESIUM-ALUMINUM ALLOY

An Optical and SEM image of the microstructure of the untreated Magnesium-Aluminum alloy was shown in Figure 2a and 2b respectively. The untreated Magnesium-Aluminum alloy showed a dendritic structure of α- Mg matrix, β-phase ($Mg_{17}Al_{12}$) and eutectic (α+β) (small globules) phases. They are mainly produced during solidification process. The β-phase ($Mg_{17}Al_{12}$) and eutectic (α+ β) phases were precipitated discontinuously at the grain boundaries as observed in Figure. 2a and 2b which is also confirmed by A. Hutter (Hütter et al. 2016).

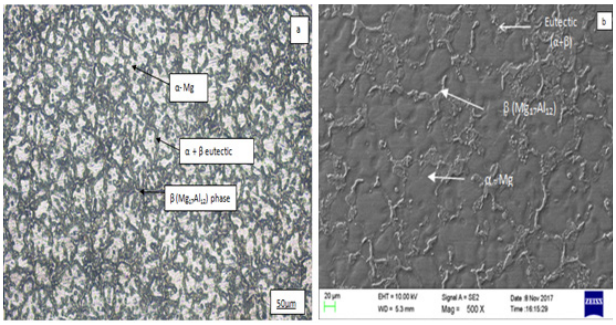


FIGURE 2. Untreated cast Magnesium-Aluminum alloy a) Optical micrograph b) SEM image in BSE mode

FSPed Magnesium-Aluminum alloy specimens without Al powder and processed with single pass at 380 and 545 rpm are shown in Figure. 3-a and 3-b respectively. It was observed that the distribution of α-Mg and β-phases ($Mg_{17}Al_{12}$) were not homogenous. This is because recrystallization of α grains took place first and then the splitted β-($Mg_{17}Al_{12}$) phase latter combined together at α-Mg matrix grain boundary because of stronger deformation. During FSP, the soft α grains were plastically deformed in the FSP direction, while the hard eutectic α + β- phase ($Mg_{17}Al_{12}$) and β-phases ($Mg_{17}Al_{12}$) prevented the α-Mg phases from deformation and the dendrites were seen to be broken at some places and also generated some branches as shown in Figure. 3-a. As the rotation speed increased during the stir pass the branches further splitted into several branches thereby reducing the average grain size of α-Mg grains as shown in Figure 3b. This is one of the reasons of α grain size was found to be smaller with higher rotation speed (545 rpm).

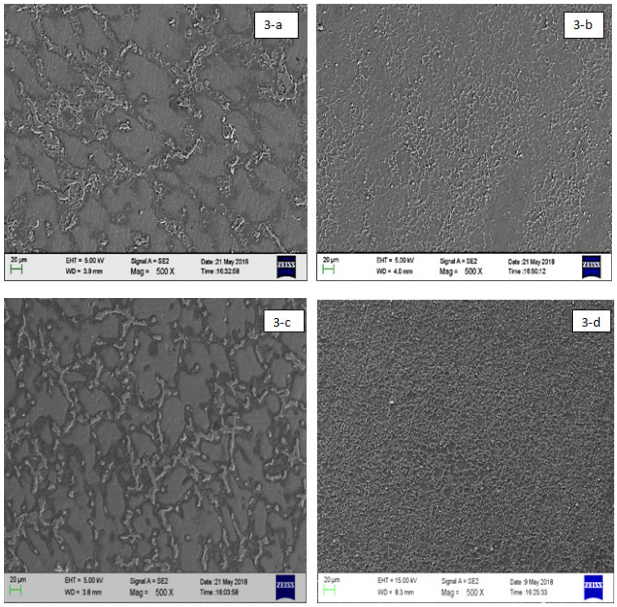


FIGURE 3. SEM images of Magnesium-Aluminum alloy FSPed without Al powder specimens a) 380 rpm with SP b) 545 rpm with SP c) 380 rpm with DP d) 545 rpm with DP

When the FSP was done with double passes at 380 and 545 rpm rotation speeds, the micrographs shown in Figure. 3-c and 3-d, respectively exhibited a homogeneous distribution of both phases together with grain refinement. Due to increase in number of passes from SP to DP, in both rotational speed 380 as well as 545 rpm, more grain refinement observed as increase in the strain in the stir zone. It can be seen that the dendrites were also similar to the die-cast alloy in 380 rpm rotational speed even after being processed by DP with little grain refinement. Further, the mechanical separations related to the refinement of α-Mg grains are mainly determined by the distribution of eutectic and β-phases ($Mg_{17}Al_{12}$). As seen in the Figure. 3-c and 3-d the eutectic phases are seen to be uniformly distributed within dendrites and even in dendritic arms. This is because the α-Mg phase is not hard compared to eutectic α + β ($Mg_{17}Al_{12}$) and β-phases ($Mg_{17}Al_{12}$) and

deformation could be done easily. Specimens processed at 380 rpm DP showed that the average grain size of α-Mg grains was smaller compared to untreated specimens (Figure. 3-c). At higher rotation speeds of 545 rpm DP, fine α-Mg grains microstructure were observed (Figure 3d). Moreover, there were also uniform distribution of β ($Mg_{17}Al_{12}$) phases resulting in higher number of α –Mg phases.

Figure 4 showed the different processed micrographs of FSPed Magnesium-Aluminum alloy by reinforcement with Al powder during both SP and DP at 380 rpm (Figure. 4-a) and 545 rpm (Figure.4-b) rpm. During the SP the Al powder is found to be distributed along the friction stir direction in the friction stirred zone. These powders were seen to be merged along with β-phases ($Mg_{17}Al_{12}$) as white particles as shown in Figure. 4a and 4b at 380 rpm rotational speed. The initial particle size of aluminum powder of ~19 µm was found to decrease in the stirred zone after friction stir processing. At higher rotation speed 545 rpm, the aluminum particles are found to occupy the spaces in α grains. As a result, a cloudy appearance was observed when the specimen were friction stirred at 545 rpm (Figure 4b). The results from EDS confirmed aluminum (Figure 6).

During the DP, the aluminum particles were found to be agglomerated and were seen as long streaked lines made of white particles. This indicates that a large number of aluminum particles are distributed along the stirred flow lines (Figure. 4-c). However, at higher rotational speed a cloudy appearance was observed as seen earlier for SP indicating that the Al particles were homogenously distributed without getting agglomerated.

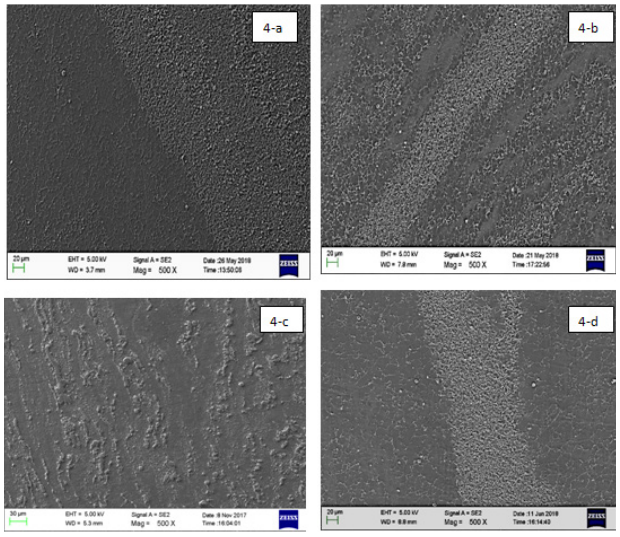


FIGURE 4. SEM images of Magnesium-Aluminum alloy FSPed with Al powder specimens at a) 380 rpm with SP b) 545 rpm with SP c) 380 rpm with DP d) 545 rpm with DP

## X-RAY DIFFRACTION PATTERNS OF UNTREATED CAST AND FSPED MAGNESIUM-ALUMINUM ALLOY

The XRD patterns for untreated cast Magnesium-Aluminum alloy and FSPed without Al powder reinforcement Mg alloys were shown in Figure. 5. It was found that the peaks corresponding to the diamond and circle symbols represented α-Mg and β-phases ($Mg_{17}Al_{12}$) respectively. Both untreated cast and FSPed specimens showed both these phases. Moreover, the intensity of α-Mg and β-phases ($Mg_{17}Al_{12}$) peaks increased after FSP. A strong refinement was attributed to the increased intensities of these processed specimens in comparison to the cast condition specimens. Comparing the processing conditions of the processed specimens, it was observed that the specimens processed at 545 rpm with both SP and DP showed higher number of α-Mg phases compared to that processed at 380 rpm. This is because there was higher grain refinement at higher rotation speeds.

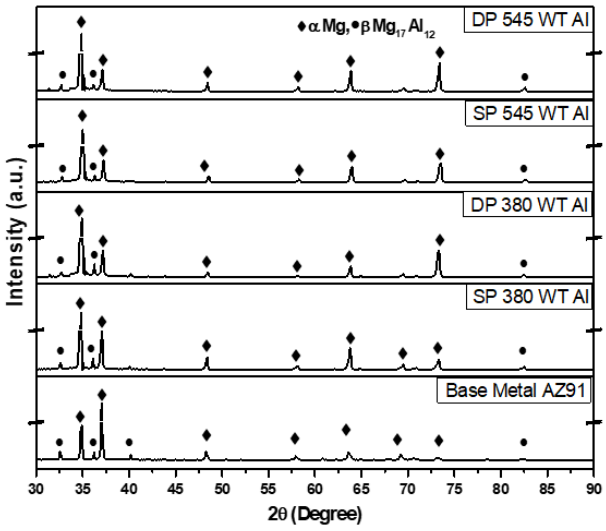


FIGURE 5. Comparison of XRD pattern of FSPed without Al powder with untreated cast Magnesium-Aluminum alloy

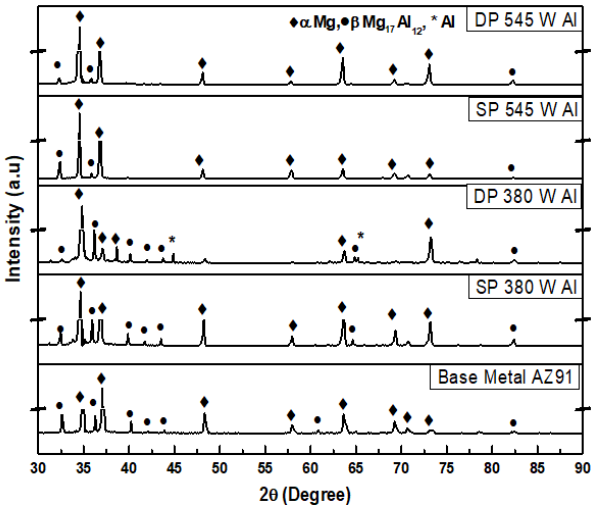


FIGURE 6. Comparison of XRD pattern of FSPed with Al powder with untreated cast Magnesium-Aluminum alloy

The XRD patterns for untreated cast Magnesium-Aluminum alloy and FSPed alloy reinforced with Al powder were shown in Figure 6. FSP specimens with Al powder showed both α-Mg, β-phase ($Mg_{17}Al_{12}$) and Aluminum phases. Moreover, the intensity of α-Mg and β-phase ($Mg_{17}Al_{12}$) peaks increased after FSP reinforced with aluminum powder. Comparing the processing conditions of the processed specimens, it was observed that the specimens processed at 380 rpm with both single and double passes showed higher amount of β-phase ($Mg_{17}Al_{12}$) phases compared to that processed at 545 rpm. No separate Al peaks are visible as they are smaller in size and their content is small to be identified in XRD patterns. However, separate peaks of aluminum were observed in the case of specimens processed by double pass at 380 rpm. This because the Al powder had agglomerated to form big particles. This is also confirmed from the SEM images as shown in Figure. 4-c. As the rotational speed increased very few peaks of β-phases ($Mg_{17}Al_{12}$) and high intensity α peaks are observed. It is interesting to note that there are no aluminum peaks in specimens treated at 545 rpm speeds indicating the homogeneous distribution of Al.

## ELECTRO CHEMICAL BEHAVIOR OF DIE CAST AND FSPED MAGNESIUM-ALUMINUM ALLOY

Potentiodynamic curves of untreated cast Magnesium-Aluminum alloy were compared with FSPed without Al powder processed with single pass and double pass under 380 and 545 rpm (Figure 7). These tests were carried out in 5 wt. % NaCl solution. Table 1 shows the corrosion rate derived from the Tafel extrapolation method of these polarization curves along with electrochemical parameters like corrosion potential ($E_{corr}$) and current density ($I_{corr}$).

TABLE 1. Comparison of the electrochemical parameters and corrosion rate derived from the Tafel extrapolation curves of untreated cast and FSPed specimens without Al powder t Magnesium-Aluminum alloy

| Sr. No | Specimen ID | Ecorr(V) | Icorr(μAmp) | Corrosion Rate (mpy) |
|---|---|---|---|---|
| 1 | Untreated cast Magnesium-Aluminum alloy | - 1.360 | 670.00 | $1.537 \times 10^3$ |
| 2 | Magnesium-Aluminum alloy FSP 380 SP without A | -1.400 | 146.00 | $3.787 \times 10^2$ |
| 3 | Magnesium-Aluminum alloy FSP 380 DP without Al | -1.380 | 165.00 | $3.362 \times 10^2$ |
| 4 | Magnesium-Aluminum alloy FSP 545 SP without Al | -1.560 | 364.00 | $8.348 \times 10^2$ |
| 5 | Magnesium-Aluminum alloy FSP 545 DP without Al | -1.310 | 46.00 | $1.055 \times 10^2$ |

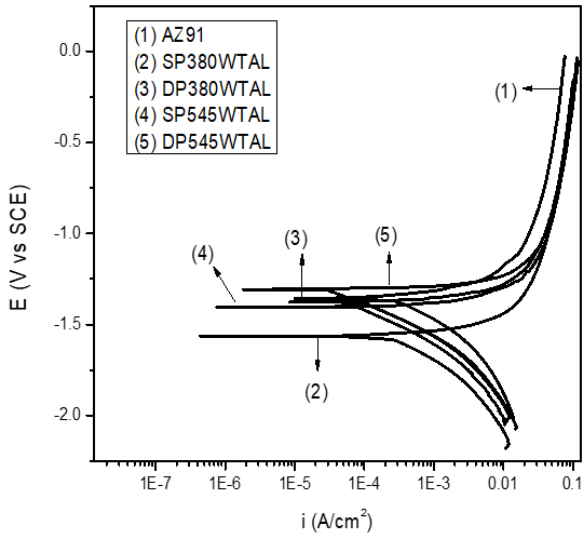


FIGURE 7. Comparison of potetiodynamic curves of FSPed Magnesium-Aluminum alloy without Al powder SP and DP with 380 and 545 rpm with untreated cast Magnesium-Aluminum alloy

As shown in Figure.7 and Table 1, the untreated cast Magnesium-Aluminum alloy shows the highest corrosion rate (Curve 1). Single pass FSP specimens have corrosion rate by an order of one magnitude less than the untreated cast alloy(curve 2and 4). While the FSPed DP specimens exhibited lower corrosion, rate compared to the SP specimens with respect to their processing rotation speeds (curve 3and 5). The poor corrosion rate of untreated cast Magnesium-Aluminum alloywas attributed to the corrosion which preferentially begins at the regions where the β-phase ($Mg_{17}Al_{12}$) was discontinuously distributed at the grain boundary of α - Mg matrix. However during FSP, asgrain refinement and dissolution of β-phases ($Mg_{17}Al_{12}$) occurs, there is an improvement in the resistances to corrosion for both SP and DP FSPed specimens. As the rotational speed increased to 545 rpm, during the double pass, more grain refinement of α-grains accompanied with more dissolution of β-phases ($Mg_{17}Al_{12}$) occurred. This led to an improvement in the corrosion resistance as indicated by the lowest Icorr and corrosion rate values. Thus, highest improvement in corrosion resistance in DP FSP at 545 rpm

specimens were due to the modification of the surface by friction stir processing at higher rotational speed and double passes.

Potentiodynamic curves of untreated cast Magnesium-Aluminum alloy were compared with FSPed Magnesium-Aluminum alloy with Al powder processed with single pass and double pass under 380 and 545 rpm was shown in Figure. 8. These tests were carried out in 5 wt. % NaCl solution. Table 2 show the corrosion rate derived from the Tafel extrapolation method of these polarization curves along with electrochemical parameters like corrosion potential ($E_{corr}$) and current density ($I_{corr}$).

TABLE 2. Comparison of the electrochemical parameters and corrosion rate derived from the Tafel extrapolation curves of untreated cast and FSPed specimens with Al powder Magnesium-Aluminum alloy

| Sr. No | Specimen ID | Ecorr(V) | Icorr(μAmp) | Corrosion Rate (mpy) |
|---|---|---|---|---|
| 1 | Untreated cast Magnesium-Aluminum alloy | -1.360 V | 670.00 | 1.537 X $10^3$ |
| 2 | Magnesium-Aluminum alloy FSP 380 SP with A | -1.370 | 102.00 | 2.346 X $10^2$ |
| 3 | Magnesium-Aluminum alloy FSP 380 DP with Al | -1.360 | 48.60 | 1.10 X $10^2$ |
| 4 | Magnesium-Aluminum alloy FSP 545 SP with Al | -1.530 | 236.00 | 5.423 X $10^2$ |
| 5 | Magnesium-Aluminum alloy FSP 545 DP with Al | -0.746 | 26.30 | 0.603 X $10^2$ |

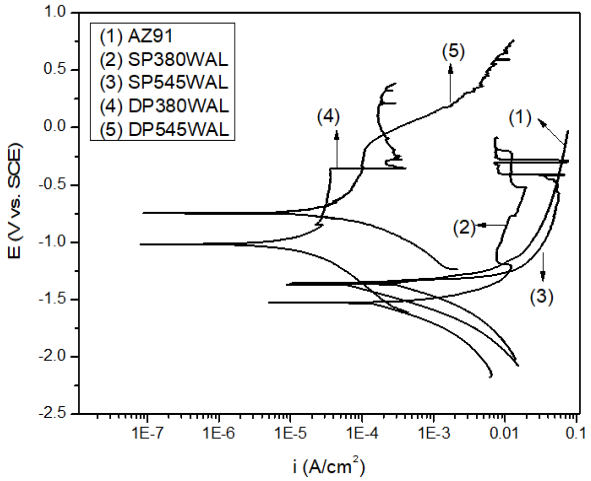


FIGURE 8. Comparison of potetiodynamic curves of FSPed Magnesium-Aluminum alloy with Al powder SP and DP with 380 and 545 rpm with untreated cast Magnesium-Aluminum alloy.

As shown in Figure 8, polarization curve 4 and 5 (FSP DP 380 and 545 with Al powder) shows better corrosion resistance than curve 3 and 2 (FSP SP 380 and 545 rpm with Al powder). During FSP with Al powder, Al powder dissolved into the β-phases ($Mg_{17}Al_{12}$) as well as in α- Mg phase because of increase in frictional heat and temperature during FSP. Thus, rise in solubility of Al in α-Mg and β-phases ($Mg_{17}Al_{12}$) improved corrosion resistance. The high Al content in α-Mg phase and more β-phases ($Mg_{17}Al_{12}$) volume acted as a barrier to minimize corrosion. This aluminum might have formed a passive layer (Al2O3) on the surface during the potentiodynamic test. The passivation region in the polarization curves of these specimens were a pure indication of this phenomenon. FSPed SP with aluminum powder curve 2 and 3 does not show significant passivation and hence shows lower corrosion resistance compared to the former specimens. Hence, least corrosion rate was observed in FSP DP 545 and 380 rpm with aluminum specimens which were also verified by their lowest Icorr values.

Thus, amongst all the FSP Magnesium-Aluminum alloy specimens, the corrosion resistance was better in FSP specimens processed under DP at 545 rpm with aluminum powder. This is mainly due to the homogeneous stirred zone enriched with aluminum obtained by double pass at 545 rpm.

## CONCLUSIONS

1. On untreated cast Magnesium-Aluminum alloy, FSP without Al and FSP with pure Al powder (average particle size ~19 μm) were done successfully .
2. FSPed DP specimens prepared with Alpowder at 545 rpm exhibited the best corrosion resistance compared to other FSPed and untreated cast Magnesium-Aluminum alloy . By addition of pure aluminum powder in FSP, it was found that the high Al particles in α- Mg phase and more β-phases ($Mg_{17}Al_{12}$) volume impede deterioration by corrosion.
3. Microstructure analysis proved that, by FSP SP specimens grain refinement achieved compared to untreated cast Magnesium-Aluminum alloy and with FSP DP specimens , severe grain refinement achieved which benefit for improvement in corrosion as more β-phases ($Mg_{17}Al_{12}$) which act as barrier to reduce corrosion compared to untreated cast Magnesium-Aluminum alloy .

4. FSP DP with Al powder, by dissolution of β-phase ($Mg_{17}Al_{12}$) minimizing the local galvanic corrosion of α-Mg and β-phases ($Mg_{17}Al_{12}$) effectively.

ACKNOWLEDGEMENT

Authors are thankful to Mechanical Department team, PDPU, for the providing facility of FSP. Authors are thankful to FCIP, Gandhinagar for providing SEM and Corrosion laboratory facilities with keen technical guidance.

DECLARATION OF COMPETING INTEREST

None

REFERENCES

Abdelaziz, M. H, Paradis, M., Samuel, A. M. Doty, H. W. , Samuel, F. H. 2017. Effect of aluminum addition on the microstructure, tensile properties, and fractography of cast mg-based alloys. *Advances in Material Science and Engineering* 2017.

Adentula, A. and Akinlabi, E. 2018. Influence of reinforcements in friction stir processed magnesium alloys: Insight in medical applications. *Material Research Express* 6(2): 025406.

Ahmadkhaniha , D., Järvenpää, A., Jaskari , M., Sohi, H., Zarei Hanzaki, A., Fedel , M., Deflorian , F., Karjalainen, L. P. 2016. Microstructural modification of pure Mg for improving mechanical and bio corrosion properties, *Journal of the Mechanical Behavior of Biomedical Materials* 61: 360-370.

Akinwekomi, A., Akinwekomi, D., Law, W. C., Choy, M. T., Chen, L., Tang, C-Y., Tsui, G. & Yang, X. 2018. Processing and characterization of carbon nanotubes reinforced magnesium alloy composite foams by rapid microwave sintering. *Material Science and Engineering: A* 726: 82–92.

Ambat, R., Aung, N., Zhou, W. 2000. Evaluation of microstructural effect on corrosion behavior of AZ91D magnesium alloy. *Corrosion Science* 42:1433-1455.

Chang, C. I., Dua, X. H., Huang, J. C. 2007. Achieving ultrafine grain size in Mg-Al-Zn alloy by friction stir processing. *Scripta Materialia* 57(3): 209-212.

Chen, T., Zhu, Z., Yuan, L., Ying, M.A., Yuan, H. 2010. Friction stir processing of thixoformed AZ91D magnesium alloy a fabrication of Al-rich surface. *Transaction of Non-Ferrous Metals Society of China* 20(1): 34-42.

Chen, T.J., Yongkun, M., Li, B., Li, Yuzhou Hao 2009, Effects of processing parameters on wear behaviors of thixoformed AZ91D magnesium alloys. *Materials and Design* 30(2):235-244.

Dani, M.S., Dave, I. B., Parmar, B. 2019, Corrosion behavior of die-cast, friction stir processed AZ91 Magnesium alloy in 5% NaCl. *Journal of The Institution of Engineers (India): Series D* 100(1): 21-27.

DU, X. H., WU, B. L. 2008. Using friction stir processing to produce ultrafine-grained microstructure in AZ61 magnesium alloy. *Transaction of Non-Ferrous Metals Society of China*, 18: 562-565.

Emley, E. F. 1966. *Principle of Magnesium Technology.* London: Pergamon Press.

Gandra, J., Miranda, R. M., Vilaca, P. 2011. Effect of overlapping direction in multi pass friction stir processing. *Materials Science and Engineering A,* 528: 5593-5599

Khodabakhshi, F., Arab, S. M., Gerlich, A. P. 2017. Materials Characterization Fabrication of a new Al-Mg/ grapheme nanocomposite by multi-pass friction-stir processing: Dispersion, microstructure, stability, and strengthening, *Materials Characterization* 132: 92–107.

Kubota, K., Mabuchi, M., Higashi, K. 1999, Processing and mechanical properties of fine-grained magnesium alloys. *Journal of Materials Science* 34(10): 2255–2262.

Hütter, A., Huemer, W., Ramskogler, C. & Warchomicka, F. 2016. Surface modification of pure magnesium and magnesium alloy AZ91 by friction stir processing, *Key Engineering Materials* 651:796-801

Li, W., Niu ,P.L., Yan, S.R., Patel, V. & Wen, Q. 2019. Improving microstructural and tensile properties of AZ31B magnesium alloy joints by stationary shoulder friction stir welding. *Journal of Manufacturing Processes* 37: 159-16.

Morisada, Y., Fujii, H., Nagaoka, T. & Fukusumi, M. 2006. MWCNTs/AZ31 surface composites fabricated by friction stir processing. *Material Science and Engineering: A* 419: 344-348.

Morisada, Y., Fujii, H., Nagaoka, T. & Fukusumi, M. B. 2006. Nano crystallized magnesium alloy-uniform dispersion of C60 molecules. *Scripta Materialia* 55: 1067-1070.

Morisada, Y., Fujii, H., Nagaoka, T., Nogi, K., Fukusumi, M. 2007. Fullerene/A5083 composites fabricated by material flow during friction stir processing. *Composites: Part A Scripta Materialia* 38: 2097-2101.

Nia, A.A., Omidvar, H. & Nourbakhsh, S.H. 2014. Effects of overlapping multi-pass friction stir process and process and rapid cooling on the mechanical properties and microstructure of AZ31 magnesium alloy. *Materials and Design* 58: 298-304.

Patel ,V., Li,W. & Xu, Y. 2018. Stationary shoulder tool in friction stir processing: a novel low heat input tooling system for magnesium alloy. *Material and Manufacturing Process:* 177182.

Patel, V., Li,W., Vairis, A ., Badheka, V . 2019. Recent development in friction stir processing as a solid-state grain refinement technique. *Critical review in Solid state and Material Sciences* 44(5): 378-426

Sharma, D.K., Badheka, V., Patel, V. & Upadhyay, G. 2021. Recent developments in hybrid surface metal matrix composites produced by friction stir processing: A review. *ASME Journal of Tribology* 143(5): 050801.

Song, G. & Atrens, A. 1999. Corrosion mechanisms of magnesium alloys. *Advance Engineering Materials* 1: 11-33.

Song, G., Atrens, A. & Dargusch, M. 1999, Influence of microstructure on the corrosion of die cast AZ91D, *Corrosion Science* 41: 249-273.

Song, G., Atrens, A., Wu, X. L. & Zhang, B. 1998. Corrosion behavior of AZ21, AZ501 and AZ91D in sodium chloride. *Corrosion Science* 40: 1769-1791.